RADIATION RESEARCH **186**, 235–244 (2016)
0033-7587/16 $15.00

DOI: 10.1667/RR14263.1

Transcript Analysis for Internal Biodosimetry Using Peripheral Blood from Neuroblastoma Patients Treated with ^{131}I-mIBG, a Targeted Radionuclide

David A. Edmondson,[a] Erin E. Karski,[b] Ayano Kohlgruber,[c] Harsha Koneru,[c] Katherine K. Matthay,[b] Shelly Allen,[b] Christine L. Hartmann,[c] Leif E. Peterson,[d] Steven G. DuBois[b] and Matthew A. Coleman[c,e,1]

[a] *School of Health Sciences, Purdue University, West Lafayette, Indiana 47907;* [b] *Department of Pediatrics, University of California San Francisco School of Medicine, San Francisco California 94143;* [c] *Lawrence Livermore National Laboratory, Livermore, California 94550;* [d] *Center for Biostatistics, Houston Methodist Research Institute. Houston, Texas 77030; and* [e] *Department of Radiation Oncology, University of California Davis, School of Medicine, Davis, California 95817*

Edmondson, D. A., Karski, E. E., Kohlgruber, A., Koneru, H., Matthay, K. K., Allen, S., Hartmann, C. L., Peterson, L. E., DuBois, S. G. and Coleman, M. A. Transcript Analysis for Internal Biodosimetry Using Peripheral Blood from Neuroblastoma Patients Treated with ^{131}I-mIBG, a Targeted Radionuclide. *Radiat. Res.* 186, 235–244 (2016).

Calculating internal dose from therapeutic radionuclides currently relies on estimates made from multiple radiation exposure measurements, converted to absorbed dose in specific organs using the Medical Internal Radiation Dose (MIRD) schema. As an alternative biodosimetric approach, we utilized gene expression analysis of whole blood from patients receiving targeted radiotherapy. Collected blood from patients with relapsed or refractory neuroblastoma who received ^{131}I-labeled metaiodobenzylguanidine (^{131}I-mIBG) at the University of California San Francisco (UCSF) was used to compare calculated internal dose with the modulation of chosen gene expression. A total of 40 patients, median age 9 years, had blood drawn at baseline, 72 and 96 h after ^{131}I-mIBG infusion. Whole-body absorbed dose was calculated for each patient based on the cumulated activity determined from injected mIBG activity and patient-specific time-activity curves combined with ^{131}I whole-body S factors. We then assessed transcripts that were the most significant for describing the mixed therapeutic treatments over time using real-time polymerase chain reaction (RT-PCR). Modulation was evaluated statistically using multiple regression analysis for data at 0, 72 and 96 h. A total of 10 genes were analyzed across 40 patients: *CDKN1A*; *FDXR*; *GADD45A; BCLXL*; *STAT5B*; *BAX*; *BCL2*; *DDB2*; *XPC*; and *MDM2*. Six genes were significantly modulated upon exposure to ^{131}I-mIBG at 72 h, as well as at 96 h. Four genes varied significantly with absorbed dose when controlling for time. A gene expression biodosimetry model was developed to predict absorbed dose based on modulation of gene transcripts within whole blood. Three transcripts explained over 98% of the variance in the modulation of gene expression over the 96 h (*CDKN1A*, *BAX* and *DDB2*). To our knowledge, this is a novel study, which uses whole blood collected from patients treated with a radiopharmaceutical, to characterize biomarkers that may be useful for biodosimetry. Our data indicate that transcripts, which have been previously identified as biomarkers of external exposures in *ex vivo* whole blood and *in vivo* radiotherapy patients, are also good early indicators of internal exposure. However, for internal sources of radiation, the biokinetics and physical decay of the radionuclide strongly influence the gene expression.

INTRODUCTION

Dose estimation after the administration of therapeutic radionuclides presents unique challenges. The practice of calculating internal radiation dose is done by either bioassay (such as urine or fecal samples) or by estimation based on activity administered, using biokinetic models as provided by the Committee on Medical Internal Radiation Dose (MIRD). While dosimeters can be used to measure dose externally, the development of a dosimeter to assess internal dose is needed. We hypothesized that the use of transcriptional assays to monitor changes at the molecular level and measurement of dose-response characteristics after irradiation might be a feasible approach towards characterizing internal biodosimetry (*1*).

Over the last two decades genome-scale tools have helped to identify large-scale changes in gene expression profiles within minutes to hours after irradiation, and have shown that a broad variety of biological pathways are modulated (*2–5*). These studies have proven useful for predicting panels of transcripts that may be beneficial for biodosimetry (*3, 4, 6–15*). However, most of these studies have been primarily focused on external irradiation. Recently, several groups have looked at internal radiation exposures with an emphasis on the mouse model (*16–19*). Internal radiation

Editor's note. The online version of this article (DOI: 10.1667/RR14263.1) contains supplementary information that is available to all authorized users.

[1] Address for correspondence: School of Medicine, Department of Radiation Oncology, University of California Davis, Sacramento, CA 95817. e-mails: mcoleman@ucdavis.edu and coleman16@llnl.gov.

TABLE 1
Patient Characteristics

	Number of patients
Total number of patients	40
Sex	
Female	10
Male	30
Concomitant radiation sensitizer	
Irinotecan + vincristine:	19
Vorinostat	7
None	14
Disease status prior to treatment	
Relapsed	18
Refractory	22
Age at treatment	
Median	7 years
Range	3–30 years
Patient weight	
Mean	31.2 kg
SD	21.2
^{131}I-mIBG administered activity	
First treatment	
Mean	17.232 mCi/kg
SD	1.5
Second treatment	
Mean	17.8 mCi/kg
SD	1.2

studies in humans have been focused on biomarkers of multiple organ damage, but have not been specifically directed toward looking for DNA damage-related responses in peripheral blood (*20–23*), where biomarkers of dose response may circulate (*10, 15, 24–31*). Characterization of known radiation-responsive transcript profiles for therapeutic radionuclides may also be useful in both the clinic and triage setting as biodosimeters.

One radiopharmaceutical of interest is iodine-131 conjugated with metaiodobenzylguanidine (^{131}I-mIBG), which is used in patients with advanced neuroblastoma that have poor outcomes. MIBG is a norepinephrine analogue that is quickly taken up by neuronal-derived cancer cells expressing the norepinephrine transporter (*32, 33*). A total of 90% of all neuroblastoma tumors are mIBG-avid (*32, 34*), such that targeted radiotherapy with ^{131}I-mIBG can be used in the majority of these patients. For patients with relapsed or refractory high-risk neuroblastoma, targeted radiotherapy is often the therapy of choice. Recent efforts have focused on combining ^{131}I-mIBG with potential radiosensitizers, such as vorinostat (*35, 36*) or irinotecan (*37*). Currently, there are also cooperative group studies underway evaluating whether incorporating ^{131}I-mIBG into upfront treatment is beneficial in cancer treatment.

When ^{131}I-mIBG is used as part of targeted radiotherapy, the mIBG is rapidly taken up by neuroblastoma tumors with a peak at approximately 6 h (*32*). This rapid clearing from the blood causes approximately 10% to remain in the blood stream within a few hours after treatment (*32*). It has also been shown that approximately 15% immediately exits the body through the bladder (*38–40*). Therefore, during the course of treatment, the patient is being exposed to an exponentially decreasing radioactive source that is both eliminated from the body and radioactively decaying. While the majority of the biodosimetry studies have been done using external radiation (*2–14, 29, 41*), patients receiving radiopharmaceuticals may be suitable models for internal biodosimetry studies.

The current study provides the opportunity to assess biological response to ionizing radiation from an exponentially decaying source from within the human body. The findings from this work may prove useful during triage after a ''dirty bomb'' explosion in a densely populated area, or where the release of a radioactive isotope would present more of an internal concern. In this study, we combined physical and biological dosimetry for the first time in patients receiving a targeted radionuclide therapy. We assessed expression of a panel of radiation response genes in the peripheral blood. Our goal was to describe the change in expression of these genes after ^{131}I-mIBG therapy and to determine the extent to which expression of these genes correlated with estimated whole-body radiation dose.

MATERIALS AND METHODS

Patient Recruitment and ^{131}I-mIBG Therapy

Patients were recruited for this pilot evaluation of novel radiation biomarkers from among individuals with relapsed or refractory neuroblastoma treated with ^{131}I-mIBG at the University of California San Francisco School of Medicine (UCSF; Table 1). Patients with relapsed and refractory neuroblastoma receiving mIBG treatment at UCSF were eligible to participate. All patients had MIBG-avid neuroblastoma by ^{123}I-mIBG diagnostic scans and were required to be older than 24 months of age. Based on availability of specific clinical trials, patients received either ^{131}I-mIBG as a single agent or ^{131}I-mIBG with either vorinostat or with vincristine and irinotecan. Patients were treated with ^{131}I-mIBG infusion over 90–120 min at UCSF, with the usual thyroid blockade and bladder protection using a bladder catheter (*37*). All patients consented to gene expression studies. This study was approved by the UCSF Committee on Human Research and the Institutional Review Boards at University of California Davis and Lawrence Livermore National Laboratory.

Blood Sample Processing

A total of 2.5 ml per time point of peripheral blood was drawn using PAXgene™ RNA blood tubes (QIAGEN®, Valencia, CA) at baseline, 72 and 96 h after ^{131}I-mIBG treatment. Blood tubes were kept at −80°C for 30 days after treatment to ensure all ^{131}I had decayed below background levels prior to isolation and analysis. The RNA was then extracted from whole blood using the PAX Gene Kit following the manufacturer's instructions. RNA was stored at −80°C until ready for use. RNA was quantified using a NanoDrop ND 1000 spectrophotometer (NanoDrop Technologies, Wilmington, DE) and Qubit® Fluorometer (Invitrogen™, Carlsbad, CA). RNA quality was checked using an Experion™ analyzer (Bio-Rad, Hercules, CA).

Gene Selection for Biodosimetry

Table 2 list genes that were selected based on prior performance in previously conducted and published gene expression experiments that emphasized robust dose-responsive transcripts (*26, 28, 29, 42, 43*) for validation in our model system. *GAPDH* was chosen as the

TABLE 2
Selected Transcripts of Interest

Gene	Name	Primer no.
GAPDH	Glyceraldehyde 3-phosphate dehydrogenase	H202758991_g1
CDKN1A	Cyclin-dependent kinase inhibitor 1A (p21)	Hs0035578_m1
FDXR	Ferrodixin reductase	Hs00244586_m1
GADD45A	Growth arrest and DNA-damage-inducible alpha	Hs00169255_m1
DDB2	Damage-specific DNA binding protein 2 (XPE)	Hs03044953_m1
XPC	Xeroderma pigmentosum, complementation group C	Hs00190295_m1
MDM2	E3 ubiquitin protein ligase	Hs00234753_m1
BCL2	B-cell CLL/lymphoma 2	Hs99999018_m1
BCLXL	BCL2-like 1	Hs00236329_m1
BAX	BCL2-associated X protein	Hs99990001_m1
STAT5B	Signal transducer and activator of transcription 5B	Hs00273500_m1

endogenous reference gene. Genes were representative of tumor suppressor protein p53 (TP53 or p53) activation of the DNA damage response pathway as well as associated signaling pathways. The apoptosis pathways included *FDXR*, *BBC3*, *BCL2*, *BCLXL*, *BAX* and *BIM*, while the cell cycle arrest domain included *CDKN1A* and *GADD45A*. The DNA repair domain was represented by *XPC* and *DDB2*.

Generation of cDNA and Real-Time PCR

For RT-PCR analysis, 200 ng of RNA was converted to single-strand cDNA using the High Capacity cDNA archive kit (Applied Biosystems®, Foster City, CA). RNA was combined with buffer, enzyme mix and RNase-free water. The reactions for cDNA synthesis were conducted using a thermocycler. Incubation was done for 1 h at 37°C, then 5 min at 95°C. cDNA was held at 4°C until it was removed and stored in a freezer between −15°C and −25°C. The cDNA was then preamplified with TaqMan® PreAmp Master Mix (Applied Biosystems). A pooled mix of TaqMan assay primers was combined with the preamp master mix. Because patients had low white blood cell levels after their treatment, 14 cycles of preamplification were done in a thermocycler to ensure that enough material was available to quantify the entire transcript panel of interest. The cycles lasted 10 min at 95°C, followed by 14 cycles of 15 s at 95°C and 4 min at 60°C.

Real-time PCR (RT-PCR) was used to quantify the expression of genes for each patient. Each reaction was performed in a volume of 20 μl and repeated in triplicate using SharkaTAQ™ Stable QPCR Master Mix (Frontier Genomics, Auke Bay, AK) and Applied Biosystems TaqMan primers (Table 2) using a 7900HT Fast Real-Time PCR System. The following PCR program was used: 10 min at 95°C, followed by 40 cycles of alternating 15 s at 95°C and 1 min at 60°C. Results from RT-PCR were in the form of cycle threshold (C_t) values, which is the cycle when amplification curves show logarithmic growth characteristics.

Physical Dosimetry Calculations

Mean absorbed dose (referred to as absorbed dose) accumulated up to each blood-collection point for each patient was calculated using standard MIRD schema similarly as previously described by Buckley *et al.* (*44*). To determine the absorbed dose for each patient during treatment, the total retention of injected activity of mIBG was first determined using a Fluke 451P Pressurized Ion Chamber radiation detector that was fixed to the ceiling above the patient for the duration of the patient's treatment. The exposure rate emitted from the patient was measured every 3 min. The measured decay curve was normalized

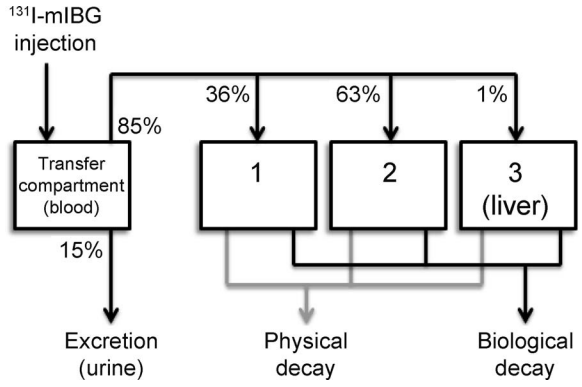

FIG. 1. A three-compartment ^{131}I-mIBG biokinetic model. This biokinetic model represents Eq. (1). The model is used for calculating dose in a patient undergoing ^{131}I-mIBG treatment. After treatment, 15% of the original injection goes straight to the bladder and is excreted. Of the remaining 85%, which is distributed among mIBG-avid tissues in the body, 1% remains in the liver until it physically decays completely, while the other 99% is shared among other tissues and processed through the two other compartments.

to injected activity to provide time-activity estimates over time for each patient (example shown in Fig. 2).

A three-compartment model (Fig. 1) was applied to the measured time-activity data for three patients using their emitted exposure rate data from the radiation detector above the bed. The effective decay constants, C_1, C_2 and C_3, representing the combined effect of physical and biological decay, were obtained for three patients where the decay constants were fitted mathematically based on the physical dosimetry data analysis from the patients, then averaged among the three patients. These effective decay constants were then used to calculate $\tilde{A}$, or the time-integrated activity, at a given time after ^{131}I-mIBG treatment, using the following equation:

$$\tilde{A} = 0.85A_o \int_0^t (C_1 e^{-\lambda_1 t} + C_2 e^{-\lambda_2 t} + C_3 e^{-\lambda_3 t})\, dt. \quad (1)$$

Equation (1) is the time-activity curve that describes the biokinetic activity of ^{131}I-mIBG in a patient. Each respective λ is the effective decay constant for each compartment, t is the time after treatment, A_o is the initial activity injected and $\tilde{A}$ is the resulting time-integrated activity at a given t. Prior empirical testing at UCSF showed that 15% of the initial injected activity is lost in the first 3 h after treatment is started, and can be assumed to be lost immediately to the urinary system and through the catheter.

The mean absorbed dose, $D_{WB\leftarrow WB}$ (in Gy) was calculated as the product of the cumulated activity and the MIRD whole-body to whole-body S value.

$$D_{WB\leftarrow WB} = \tilde{A} \times S_{WB\leftarrow WB} \quad (2)$$

As shown by Amundson *et al.* (*43*), $S_{WB\leftarrow WB}$ values were corrected for the weight of each child, using Eq. (3). Since these are calculated using an adult as a reference individual, S values were recalculated using the following equation to take into account the differences in size for each child in the study:

$$S_{WB\leftarrow WB}\left(\frac{Gy}{MBq \cdot hr}\right) = 1.34 \times 10^{-4} m_{patient}^{-0.921}, \quad (3)$$

where $m_{patient}$ is the mass of the patient in kilograms. This equation was generated by interpolating the $S_{WB\leftarrow WB}$ values from the MIRD phantoms for a newborn; for 1-, 5-, 10- and 15-year-old children; and for an adult, each of which has a specific mass (*44, 45*).

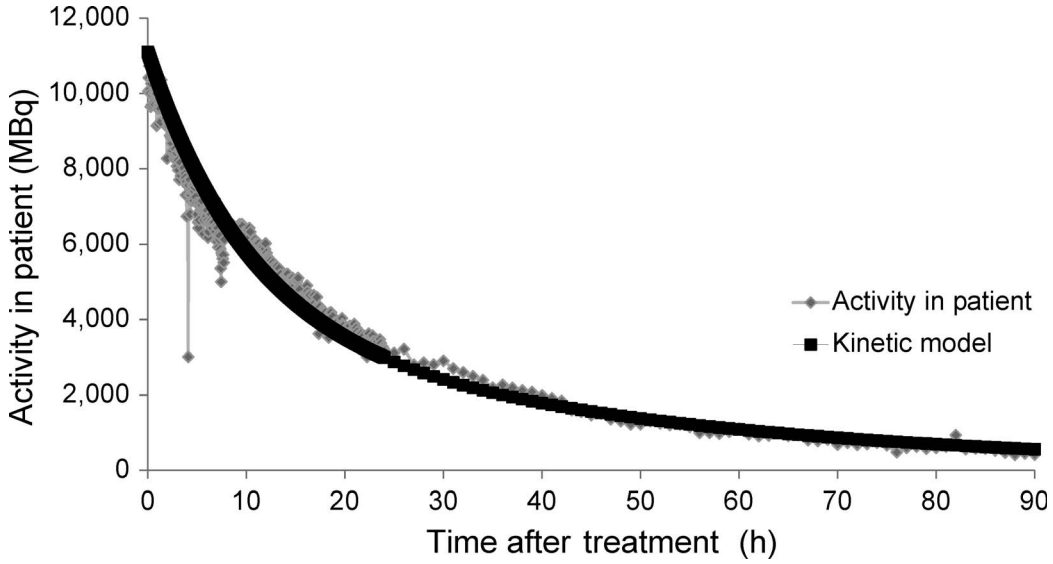

FIG. 2. An example of exponential decay of ^{131}I within a single patient. ^{131}I-mIBG, as well as other radionuclides, are eliminated by two major processes within the human body: physical decay and biological decay (elimination). The amount of activity in the patient is derived from comparing the amount of activity injected to the peak dose rate given off by the patient. Due to patient movement, distance from the radiation detector changes, resulting in dose-rate fluctuations. The data is drawn on a time plot and used to estimate total dose. The black line represents the calculated amount of activity remaining in the patient at a given time based on the kinetic model. Diamond-shaped symbols represent the calculated activity in the patient based on dose rate, which is measured by the meter mounted on the ceiling above the patient.

Absorbed doses calculated as above are referred to as kinetic model-based doses (KM dose) in this study.

Statistical Methods

Fold change was calculated with the $2^{-\Delta\Delta Ct}$ method as described by Livak and Schmittgen (*46*), using C_t values as determined from the RT-PCR analysis using absolute quantification. A C_t value is inversely proportional to the amount of material in a sample; the higher the C_t the less amount of material. Multiple linear regression was used to assess the effect of time since treatment, absorbed dose and concomitant radiation sensitizer exposure on gene expression. Welch *t* tests, which assumed unknown variance, were performed to compare differences between serial treatments for patients who received more than one treatment. To determine which variables contributed most to the variance explanation in dose-dependent fold change, backward stepwise regression analysis was performed using $P < 0.05$ for variable entry. A significance level of $\alpha = 0.05$ was used for all tests. A *P* value of 0.05 was used for determining significance. All analyses were conducted using the R environment (*47*).

RESULTS

Patient Characteristics

Characteristics of the 40 patients who participated in this pilot study are shown in Table 1. There were 30 males and 10 females. A total of 14 patients received mIBG treatment only, while 19 patients received vincristine/irinotecan and 7 received vorinostat in combination with mIBG. Nine patients received a second mIBG treatment approximately 6 weeks after the initial treatment. Our analysis focused only on the effects in patients that were associated with radiation dose and time for mIBG treatment within the first 96 h after exposure to demonstrate the utility of our approach. In addition, 6 of the patients lacked complete dosimetry information after the initial exposure and these were used for testing our exposure model.

Modulation of Gene Expression after ^{131}I-mIBG Treatment

All 10 transcripts of interest gave measurable baseline signals in the RT-PCR assays. The expression levels of 9 transcripts were significantly altered compared to controls after mIBG treatment (Supplementary Table S1; http://dx.doi.org/10.1667/RR14263.1.S1). Figure 3 shows the change in translation over the course of 72 and 96 h from baseline. The transcripts *CDKN1A*, *FDXR*, *GADD45A*, *STAT5B*, *BAX*, *XPC*, *MDM2* and *DDB2* were significantly upregulated at 72 h as well as at 96 h while *BCLXL* was significantly downregulated at 72 h. *MDM2* was the only transcript that was upregulated at 72 h and returned to baseline within the first 96 h. Interestingly, the *BCLXL* transcript was more significantly downregulated with a lower fold change at the 96 h time point compared to 72 h postirradiation. The *BCL2* transcript did not show modulated expression in our study.

Significance of Differential Transcript Response Varied with Dose and Time

Multiple regression analyses were performed to determine the significance of the effects of dose and elapsed time after treatment on each transcript. All fold changes

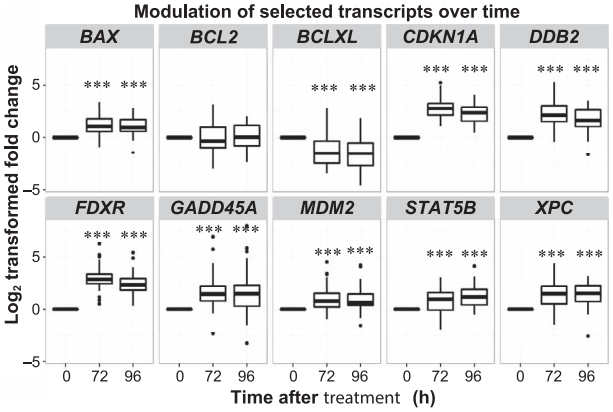

FIG. 3. Box-whisker plots show the modulation of selected transcripts over time. This collection of plots shows the changes in gene expression at each time interval after ^{131}I-mIBG treatment. The x-axis shows the time points sampled (0–96 h), while the y-axis shows the transformed $\log_2$ fold change of expression levels. The transcripts *BAX*, *CDKN1A*, *DDB2*, *FDXR*, *GADD45A*, *MDM2*, *STAT5B* and *XPC* show time-dependent upregulation while *BCLXL* shows time-dependent downregulation (paired Student's *t* test vs. 0 h after treatment, ***$P < 0.001$). *BCL2* did not have a time-dependent response to radiation.

used were $\log_2$ transformed to normalize the expression around 0 for statistical testing. Concomitant drug treatment (vorinostat or vincristine/irinotecan) was used as a control variable, but was not included in the final analysis, to keep the focus on the effects of dose from the mIBG treatment alone. Table 3 shows the results of where the values are the β for each parameter while values in parentheses are standard error. The β values represent slopes of the regression line where a positive value represents increasing expression while a negative value represents decreasing expression. Due to the varying modulation of transcripts between 72 and 96 h, these results demonstrated a time dependency that needs to be taken into account for generating dose-related models.

A Best-Fit Gene Expression Model Defines the Three Transcripts that Best Predict Internal Dose

Based on the multiple regression analysis results, genes that presented significant differences in expression and time as a continuous variable, rather than as a factor, were analyzed in a step-wise regression analysis to determine which of these genes best described the linear change in dose over time. The lowest Akaike Information Criterion (AIC) determined the equation that best fit the data. The result of the regression showed that the response of three transcripts over the time measured described 98.7% of the variance in dose across all patients. *CDKN1A*, *BAX*, *DDB2* and time after ^{131}I-mIBG treatment contributed to describing the variance in the dose that a patient receives. This model could then be used to predict dose as a calibration equation. Values listed in Table 4 were used with Eq. (2) to determine the gene expression model-based dose.

$$E(\text{Dose}|CDKN1A + BAX + DDB2 + \text{h}) = 11.16(CDKN1A) - 19.44(BAX) + 13.09(DDB2) - 2.75\,(\text{h}) \quad (4)$$

The β is the slope of the regression line of each gene, which describes the linear change in dose and time in relationship to the differential gene expression.

The β values in Eq. (2) were multiplied by the associated genes' $\log_2$ transformed fold changes (or elapsed hours since ^{131}I-mIBG treatment) and then summed together to give the gene expression model-based dose result. These values are referred to as the gene expression model dose (GE dose). To compare how useful a gene expression model was, a model using time as the only independent variable was used to estimate doses as well [see Eq. (3)]. Using this time-only model, at 72 h the predicted dose was 2.21 Sv, and at 96 h the predicted dose was 2.94 Sv.

TABLE 4
Best-Fit Model for GE Dose Prediction

	β value	Standard error	*P* value
CDKN1A	11.16	3.38	0.0015
BAX	–19.44	5.48	0.0007
DDB2	13.09	4.09	0.002
Hour	2.75	0.10	<2E–16

TABLE 3
Multiple Regression Analysis Results for Gene Expression Based on Dose and Time

	Intercept	Total absorbed dose	72 h	96 h
CDKN1A	0.29 (0.15)	–6E – 4 (3E – 3)	2.96[b] (0.94)	2.47[a] (1.03)
FDXR	–0.22 (0.19)	–4E – 3 (4E – 3)	4.15[c] (1.16)	3.74[b] (1.27)
GADD45A	–0.31 (0.32)	–3E – 3 (8E – 3)	2.35 (1.94)	2.43 (2.14)
BCLXL	0.80[c] (0.23)	9E – 3 (5E – 3)	–3.46[a] (1.46)	–3.92[a] (1.61)
STAT5B	–0.23 (0.17)	–3E – 4 (3E – 3)	0.86 (1.05)	1.31 (1.16)
BAX	–0.14 (0.15)	–8E – 3[a] (4E – 4)	3.19[b] (0.96)	3.28[b] (1.06)
BCL2	–0.41 (0.21)	–2E – 3 (5E – 5)	0.36 (1.32)	0.58 (1.46)
XPC	–0.50[a] (0.19)	–9E – 3 (5E – 3)	3.68[b] (1.21)	3.89[b] (1.33)
DDB2	–0.36 (0.24)	–6E – 3 (6E – 3)	3.82[a] (1.48)	3.26[a] (1.63)
MDM2	0.01 (0.23)	–2E – 3 (6E – 3)	1.72 (1.52)	1.76 (1.66)

[a] $P < 0.05$, [b] $P < 0.01$ and [c] $P < 0.001$.

TABLE 5
Comparison of KM Dose vs. GE Dose Using Best-Fit Model Equation

Patient	Hour	KM dose (Sv)	GE dose (Sv)	Prediction interval (95%) (Sv)	Absolute percentage difference between KM and GE doses
1	72	2.64	2.49	2.00–2.97	5.71%
1	96	2.91	3.05	2.57–3.53	4.74%
1[a]	72	2.63	2.32	1.84–2.80	11.86%
1[a]	96	2.91	2.99	2.51–3.47	2.81%
2	72	2.56	2.11	1.63–2.60	17.66%
2	96	2.83	2.84	2.33–3.39	0.44%
3	72	2.78	2.86	2.33–3.39	2.86%
3	96	3.07	3.43	2.92–3.94	11.84%
4	72	2.43	2.47	1.98–2.95	1.68%
4	96	2.68	2.89	2.41–3.38	8.04%
5	72	2.82	1.94	1.45–2.44	31.19%
5	96	3.12	2.93	2.45–3.41	6.14%
6	72	2.77	2.54	2.05–3.04	8.11%
6	96	3.05	2.87	2.38–3.35	6.12%

[a] Second treatment for patient.

$$E(\text{Dose}|\text{hour}) = 3.07\,(\text{h}) \qquad (5)$$

Gene Expression Model Predicts Absorbed Dose for ^{131}I-mIBG Patients with Incomplete Dose Information

The best-fit model was used to estimate GE dose on six patients based only on gene expression fold change and time after ^{131}I-mIBG treatment. These six patients were selected for model fitting because they lacked complete dose information other than the total for mCi/kg of ^{131}I-mIBG injected at the start of treatment. Results are shown in Table 5. On average, the gene expression model estimated the GE dose within an absolute 8.5% of the KM dose while the model using only the hour as a predictor estimated the dose within an absolute 10.5%. Thirteen out of fourteen of the GE dose estimates were within the 95% prediction interval, while the time-only model had 11 out of 14 of the calculated doses within the 95% prediction interval (results not shown). The two models for absorbed dose (KM and GE) within a patient were compared with one another. The KM dose and GE dose were significantly correlated, suggesting that each model has similar prediction qualities for measuring the absorbed dose from a patient (Fig. 4).

Multiple mIBG Treatments did not Affect Transcript Responses

Residual treatment may be a complication due to altered transcript levels and needs to be accounted for in the study. Nine patients received two rounds of ^{131}I-mIBG therapy within this study with no shorter than one month elapsing between the treatments. Welch's two-sample *t* tests were performed to judge whether there were changes in gene expression based on prior exposure from mIBG therapy. There were no significant differences between the two treatments started at different times based on altered gene expression. Thus individuals with prior treatment could be considered as single-dosed patients.

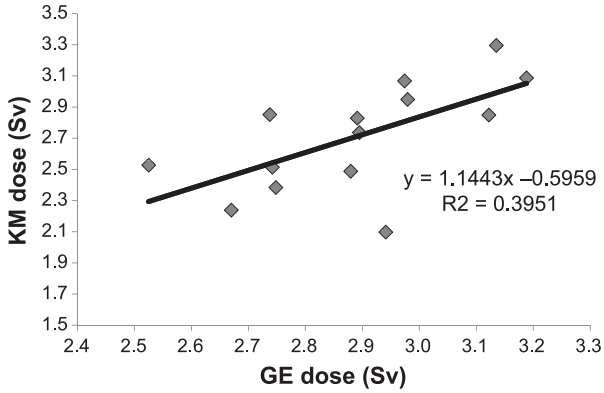

FIG. 4. Kinetic mode-based dose (KM dose) vs. gene expression-based dose (GE dose). This figure shows the relationship between GE dose from the best-fit model (Eq. 2) and the KM dose using the retention function (Eq. 1). KM dose and GE dose are collinear ($R^2 = 0.395$, $P = 0.016$) and represent similar prediction qualities for measuring absorbed dose from a patient.

DISCUSSION

Our results showed that previously identified DNA damage response and apoptosis transcripts for external radiation exposure will work as early indicators for internal exposure to ^{131}I using peripheral white blood cells. Our study also demonstrates that biodosimetry of internal radiation dose in human chemo-radiotherapeutic patients is a potential option during, as well as after treatment with internal radiotherapeutics such as mIBG, when it is possible to obtain a blood sample prior to treatment to be used as a pretreatment control. In this study we found that white blood cell gene expression after internal radiation exposure was correlated with the kinetics of dose decay rather than total absorbed dose. Interestingly, our study suggests that prior treatments were not a confounding factor as shown by analyzing nine patients with prior mIBG treatment over the time period studied. This may indicate that baseline levels for the transcripts we studied are reset within the time frame between treatments, four weeks, for our patient population. Importantly, we confirmed that a predictive model is possible based on significant differential transcript modulation associated with time after administration of a radiopharmaceutical.

These findings illustrate the potential use of DNA damage-related transcript analysis in humans, in the absence of physical dosimetry, for events involving large uncontrolled releases of radionuclides in which human and environmental uptake is probable, e.g., dirty bombs or nuclear reactor accidents. In such scenarios, since both external and internal radiation exposure would be of some consequence, developing biodosimetry for internal radiation dose could have utility for establishing triage in affected areas. Additional experiments will be necessary to elucidate

the low-dose effects and differentiate them from the higher doses measured in this current pilot study. Our data demonstrate that a small panel of responsive transcripts may be useful in such circumstances at early times to rapidly sort out the ^{131}I-exposed from unexposed individuals at doses in the range of approximately 2–3 Gy.

Using RNA in peripheral white blood cells as a biodosimeter for internal exposures is plausible for several reasons: 1. Obtaining a blood sample for testing is a relatively noninvasive procedure; 2. Blood circulates throughout the body and can be used to estimate whole-body doses; and 3. The white blood cells are well characterized in terms of DNA damage and sensitivities to radiation exposures. However, because beta-emitters (such as ^{131}I) deposit most of their emitted energy locally, e.g., within the blood, specific organs or at the tumor site, the majority of the dose is not necessarily deposited homogenously throughout the whole body. Therefore, using whole-body dose estimates as the measurement of comparison to gene expression might not be the best choice. The dose estimate can be difficult and requires consideration of biological and physical decay, as was shown in this study. There are also other issues such as self-shielding (i.e., aggregate particles absorbing emitted energy), blood flow velocity and the continually changing blood vessel geometry, which may affect the modeling (*48*). However, when samples are taken at regular intervals over a longer period of time (approximately 168 h) and the activity concentration of ^{131}I-mIBG is analyzed, estimation of total activity in the blood, and therefore dose, could be calculated. A study conducted by A. A. Yalow derived the following empirical equation:

$$D_{\text{blood}} = [0.214(B_1 - B_2)t_1] + (41.62B_2) \qquad (6)$$

Where D_{blood} is the absorbed dose to the blood, t_1 is the effective half-life of mIBG retention in the blood (h), and B_1 and B_2 are the concentration of mIBG in the first and last measurements, respectively (*49*). Flower *et al.* (*49*) calculated an absorbed dose to the blood of 0.04–0.17 mGy/MBq, whereas in this study, we calculated the absorbed dose to the blood to be between 0.01 and 0.10 mGy/MBq with a range of doses to the blood of 0.95–1.47 Gy. However, since the blood was never tested at 168 h, nor was any blood tested for activity content, the dose estimates were not used for any calculations. If patients were better monitored and sampled, it might be possible to calculate dose and develop an accurate and specific biodosimetric model, as conducted in our experiments.

We found that the genes, previously identified as potential external biodosimeters, were responsive to internal radiation exposures in humans at similar levels of expression. These results were similar to findings by Paul *et al.*, using a mouse model and gene expression arrays (*19*). Significant modulation was identified and detected up to 96 h after treatment using *CDKN1A*, *FDXR*, *BCLXL*, *BAX*, *XPC* and *DDB2* transcripts. This similarity suggests that these genes may be robust biomarkers on different types of radiation exposure routes (external and internal). Classifying the gene expression within cells after irradiation is of the upmost importance when choosing a model that best reflects the amount of energy deposited in a given biological system. In the future, it may be ideal to use array or sequencing technologies to better understand what is happening mechanistically in the peripheral blood of these cancer patients.

One notable difference between our study and previous studies (*10, 50*) was that the amount of modulation (fold change) in our study was attenuated for comparable total doses. Paul and Amundson reported that *FDXR* expression increased by about 12-fold 6 h after 2 Gy irradiation with little change after 24 h (*10*). This is in contrast to our study, which showed that the difference between 72 h (8.48-fold change) and 96 h (6.05-fold change) was approximately 2.4-fold. Manning *et al.* reported that *FDXR* increased significantly after 24 h to an approximate fold change of over 37 (*50*). This is much higher than our average fold change of 8.48 at 72 h. However, due to constraints on patient sampling, it is unknown if *FDXR* would be higher after 24 h in our study. Nevertheless, assuming *FDXR* modulation increases with increased dose, the increased dose rate at 24 h would lead one to predict a higher fold change at 24 h. This prediction necessitates further exploration into both the time dependence of gene expression for our selected panel of transcripts and how they change for internal exposures.

Nearly all genes tested were upregulated in this study and showed peak expression at 72 h with a descent in expression at 96 h. This behavior was also documented in a recent study by Tucker *et al.* (*15*) where the changes in *CDKN1A* ΔC_t for 2.5 Gy dose at 1 day vs. 2 days were carefully examined. Based on our study and Tucker's study, there are two behaviors of gene expression that require consideration in biodosimetry models.

The first behavior of concern is the dose-dependent response where greater dose causes more expression of that gene. As has been shown in studies, *CDKN1A* in particular appears to increase in expression linearly with increasing dose until it reaches a threshold around 6 Gy and then plateaus (*15, 42, 51*). This affects dose prediction, since doses greater than 6 Gy cannot be predicted with certainty (*51*). Our study, however, contradicts this. Our doses continued to increase over time, albeit due to an exponentially decaying dose rate. Nonetheless, as our dose increased, gene expression became less significant or plateaued.

The second behavior of concern is the time-dependent response: as the time lapse increases after radiation exposure, the expression of the gene should dampen. Making this more complicated are the effects of an exponentially decaying source of radiation that is persistent rather than acute. Our study took this into account by including time elapsed as a part of the equation for

predicting whole-body dose. The true cause of the time dependency in our study is most likely directly related to the exponentially decaying but ever-present radiation field acting on the white blood cells. But the entire mechanism requires further research to develop a model for comparing internal dose to external dose using similar decay parameters.

Despite increasing knowledge of genomics, there is still a need for further information on how individualized panels of biomarkers perform in unique populations and under different exposure conditions. For example, how does a dose-responsive biomarker respond to internal dose in young individuals? To address this question, our study selected DNA damage-related responsive transcripts identified in peripheral blood, where biomarkers of dose response are known to circulate. For example, *CDKN1A* is very responsive to radiation and studies have shown that its increase in behavior is close to linear with increasing dose. However, these prior studies primarily address acute, external doses, which should be useful for determining doses from whole-body radiation therapy and, possibly, criticality accidents. For targeted radiotherapy or nuclear accidents, these studies are less useful. Instead, a study like this one is needed that takes into account the exponential decay of activity after an uptake of a radionuclide. In this study, *CDKN1A* had a peak response at 72 h with a subsequent decay at 96 h (as did *FDXR* and most other genes in the study), which indicates additional data are needed to identify the longevity of the gene expression.

Fold change was used for comparison of expression in this study, but the ΔC_T value might be a simpler estimate if one can precisely control for the input quality and amount of RNA. The disadvantage of using fold change is that to calculate a difference one must have a base value. In the case of a nuclear incident, the base value would be unknown and so the fold change model would not work. A ΔC_T value compared across up and down genes may be a better indicator of exposure. More extensive testing and predictive models would need to be developed to take advantage of the ΔC_T value. With further study, a base C_T value for specific genes could be decided as a threshold, from which a quick analysis could determine if an individual had been exposed to higher levels of radiation. Nonetheless, we were able to develop a model that predicted internal dose with good precision using only three transcripts.

In summary, this study shows that even at 96 h after radiopharmaceutical treatment, the modulation in gene expression is still significant enough to discriminate between exposed and nonexposed samples using a selected gene transcript panel. We also showed how time dependency of gene expression becomes very important for internal dose estimation. Taking into account the modulation of multiple genes enables us to generate a prediction equation that could reasonably predict a patient's or exposed individual's dose in comparison to calculated methods. In addition to serving as biomarkers for internal radiation dose, these biomarkers have been incorporated into an ongoing randomized phase II clinical trial to compare different mIBG treatment regimens and to identify the paths for benefiting patient outcome in the future.

SUPPLEMENTARY INFORMATION

Table S1. Models for assessing cancer risks.

ACKNOWLEDGMENTS

We would like to thank Angela Evans for technical help with sample processing. This project was supported by the National Institutes of Health/National Cancer Institute (grant no. R01CA172067). Funding was also provided by the U.S. Department of Energy under contract no. DE-AC52-07NA27344, with funding from the U.S. DOE Low Dose Radiation Research Program, grant no. KP110202. In addition, support was provided by NIH T32 grant no. 5T32CA128583-05 awarded to UCSF Benioff Children's Hospital, and by the Campini Foundation, Alex's Lemonade Stand Foundation (MIBG Infrastructure Grant) and NIH/NCRR UCSF-CTSI grant no. UL 1 TR000004 and Columbia University NIH/NIAID pilot grant U19 AI067773.

Received: September 14, 2015; accepted: June 24, 2016; published online: August 24, 2016

REFERENCES

1. Swartz HM, Williams BB, Flood AB. Overview of the principles and practice of biodosimetry. Radiat Environ Biophys 2014; 53:221–32.
2. Snyder AR, Morgan WF. Radiation-induced chromosomal instability and gene expression profiling: searching for clues to initiation and perpetuation. Mutat Res 2004; 568:89–96.
3. Park W-Y, Hwang C-I, Im C-N, Kang M-J, Woo J-H, Kim J-H, et al. Identification of radiation-specific responses from gene expression profile. Oncogene 2002; 21:8521–8.
4. Yin E, Nelson DO, Coleman MA, Peterson LE, Wyrobek AJ. Gene expression changes in mouse brain after exposure to low-dose ionizing radiation. Int J Radiat Biol 2003; 79:759–75.
5. Amundson S, Bittner M, Chen Y. Fluorescent cDNA microarray hybridization reveals complexity and heterogeneity of cellular genotoxic stress responses. Oncogene 1999; 18:3666–72.
6. Amundson SA, Do KT, Vinikoor L, Koch-Paiz CA, Bittner ML, Trent JM, et al. Stress-specific signatures: expression profiling of p53 wild-type and -null human cells. Oncogene 2005; 24:4572–9.
7. Gruel G, Lucchesi C, Pawlik A, Frouin V. Novel microarray-based method for estimating exposure to ionizing radiation. Radiat Res 2006; 166:746–56.
8. Kimura S, Ishidou E, Kurita S, Suzuki Y, Shibato J, Rakwal R, et al. DNA microarray analyses reveal a post-irradiation differential time-dependent gene expression profile in yeast cells exposed to X-rays and gamma-rays. Biochem Biophys Res Commun 2006; 346:51–60.
9. Zhou T, Chou J, Simpson D. Profiles of global gene expression in ionizing-radiation-damaged human diploid fibroblasts reveal synchronization behind the G1 checkpoint in a G0-like state. Environ Health Perspect 2006; 114:553–9.
10. Paul S, Amundson S. Development of gene expression signatures for practical radiation biodosimetry. Int J Radiat Oncol 2008; 71:1236–44.
11. Jen K-Y, Cheung VG. Transcriptional response of lymphoblastoid cells to ionizing radiation. Genome Res 2003; 13:2092–100.

12. Otomo T, Hishii M, Arai H, Sato K, Sasai K. Microarray analysis of temporal gene responses to ionizing radiation in two glioblastoma cell lines: up-regulation of DNA repair genes. J Radiat Res 2004; 45:53–60.
13. Rieger K, Hong W. Toxicity from radiation therapy associated with abnormal transcriptional responses to DNA damage. Proc Natl Acad Sci U S A 2004; 101:6635–40.
14. Short SC, Buffa FM, Bourne S, Koritzinsky M, Wouters BG, Bentzen SM. Dose- and time-dependent changes in gene expression in human glioma cells after low radiation doses. Radiat Res 2007; 168:199–208.
15. Tucker JD, Joiner MC, Thomas RA, Grever WE, Bakhmutsky MV, Chinkhota CN, et al. Accurate gene expression-based biodosimetry using a minimal set of human gene transcripts. Int J Radiat Oncol 2014; 88:933–9.
16. Langen B, Rudqvist N, Parris TZ, Schüler E, Helou K, Forssell-Aronsson E. Comparative analysis of transcriptional gene regulation indicates similar physiologic response in mouse tissues at low absorbed doses from intravenously administered 211At. J Nucl Med 2013; 54:990–8.
17. Schüler E, Parris TZ, Rudqvist N, Helou K, Forssell-Aronsson E. Effects of internal low-dose irradiation from 131I on gene expression in normal tissues in Balb/c mice. EJNMMI Res 2011; 1:29.
18. Schüler E, Rudqvist N, Parris TZ, Langen B, Spetz J, Helou K, et al. Time- and dose rate-related effects of internal (177)Lu exposure on gene expression in mouse kidney tissue. Nucl Med Biol 2014; 41:825–32.
19. Paul S, Ghandhi SA, Weber W, Doyle-Eisele M, Melo D, Guilmette R, et al. Gene expression response of mice after a single dose of (137)cs as an internal emitter. Radiat Res 2014; 182:380–9.
20. Abend M, Pfeiffer RM, Ruf C, Hatch M, Bogdanova TI, Tronko MD, et al. Iodine-131 dose dependent gene expression in thyroid cancers and corresponding normal tissues following the Chernobyl accident. PLoS One 2012; 7:e39103.
21. Ory C, Ugolin N, Schlumberger M, Hofman P, Chevillard S. Discriminating gene expression signature of radiation-induced thyroid tumors after either external exposure or internal contamination. Genes (Basel) 2011; 3:19–34.
22. Maenhaut C, Detours V, Dom G, Handkiewicz-Junak D, Oczko-Wojciechowska M, Jarzab B. Gene expression profiles for radiation-induced thyroid cancer. Clin Oncol (R Coll Radiol) 2011; 23:282–8.
23. Bauchinger M, Schmid E, Braselmann H. Cytogenetic evaluation of occupational exposure to external g-rays and internal 241Am contamination. Mutat Res 1997; 395:173–8.
24. Ropolo M, Balia C, Roggieri P, Lodi V, Nucci MC, Violante FS, et al. The micronucleus assay as a biological dosimeter in hospital workers exposed to low doses of ionizing radiation. Mutat Res 2012; 747:7–13.
25. Knops K, Boldt S, Wolkenhauer O, Kriehuber R. Gene expression in low-and high-dose-irradiated human peripheral blood lymphocytes: Possible applications for biodosimetry. Radiat Res 2012; 178:304–12.
26. Budworth H, Snijders AM, Marchetti F, Mannion B, Bhatnagar S, Kwoh E, et al. DNA repair and cell cycle biomarkers of radiation exposure and inflammation stress in human blood. PLoS One 2012; 7:e48619.
27. Rao BS, Natarajan AT. Retrospective biological dosimetry of absorbed radiation. Radiat Prot Dosimetry 2001; 95:17–23.
28. Paul S, Smilenov LB, Amundson SA. Widespread decreased expression of immune function genes in human peripheral blood following radiation exposure. Radiat Res 2013; 180:575–83.
29. Amundson SA, Grace M, McLeland C. Human in vivo radiation-induced biomarkers Gene expression changes in radiotherapy patients. Cancer Res 2004; 64:6368–71.
30. Ivey RG, Moore HD, Voytovich UJ, Thienes CP, Lorentzen TD, Pogosova-Agadjanyan EL, et al. Blood-based detection of radiation exposure in humans based on novel phospho-Smc1 ELISA. Radiat Res 2011; 175:266–81.
31. Ory C, Ugolin N, Hofman P, Schlumberger M, Likhtarev IA, Chevillard S. Comparison of transcriptomic signature of post-Chernobyl and postradiotherapy thyroid tumors. Thyroid 2013; 23:1390–400.
32. Vöö S, Bucerius J, Mottaghy FM. I-131-MIBG therapies. Methods 2011; 55:238–45.
33. DuBois SG, Matthay KK. I-131 Metaiodobenzylguanidine therapy in children with advanced neuroblastoma. Q J Nucl Med Mol Imaging 2013; 57:53–65.
34. DuBois SG, Matthay KK. Radiolabeled metaiodobenzylguanidine for the treatment of neuroblastoma. Nucl Med Biol 2008; 35:S35–48.
35. More S, Itsara M, Yang X, Geier E. Vorinostat increases expression of functional norepinephrine transporter in neuroblastoma in vitro and in vivo model systems. Clin Cancer Res 2011; 17:2339–49.
36. Mueller S, Yang X, Sottero T, Gragg A. Cooperation of the HDAC inhibitor vorinostat and radiation in metastatic neuroblastoma: efficacy and underlying mechanisms. Cancer Lett 2011; 306:223–9.
37. DuBois SG, Chesler L, Groshen S, Hawkins R, Goodarzian F, Shimada H, et al. Phase I study of vincristine, irinotecan, and ^{131}I-metaiodobenzylguanidine for patients with relapsed or refractory neuroblastoma: a new approaches to neuroblastoma therapy trial. Clin Cancer Res 2012; 18:2679–86.
38. Matthay KK, Panina C, Huberty J, Price D, Glidden D V, Tang HR, et al. Correlation of tumor and whole-body dosimetry with tumor response and toxicity in refractory neuroblastoma treated with (131)I-MIBG. J Nucl Med 2001; 42:1713–21.
39. Matthay KK, DeSantes K, Hasegawa B, Huberty J, Hattner RS, Ablin A, et al. Phase I dose escalation of 131I-metaiodobenzylguanidine with autologous bone marrow support in refractory neuroblastoma. J Clin Oncol 1998; 16:229–36.
40. Koral KF, Huberty JP, Frame B, Matthay KK, Maris JM, Regan D, et al. Hepatic absorbed radiation dosimetry during I-131 metaiodobenzylguanidine (MIBG) therapy for refractory neuroblastoma. Eur J Nucl Med Mol Imaging 2008; 35:2105–12.
41. Paul S, Smilenov LB, Elliston CD, Amundson SA. Radiation dose-rate effects on gene expression in a mouse biodosimetry model. Radiat Res 2015; 184:24–32.
42. Wyrobek A, Manohar C. Low dose radiation response curves, networks and pathways in human lymphoblastoid cells exposed from 1 to 10 cGy of acute gamma radiation. Mutat Res 2011; 722:119–30.
43. Amundson SA, Myers TG, Fornace AJ. Roles for p53 in growth arrest and apoptosis: putting on the brakes after genotoxic stress. Oncogene 1998; 17:3287–99.
44. Buckley SE, Chittenden SJ, Saran FH, Meller ST, Flux GD. Whole-body dosimetry for individualized treatment planning of 131I-MIBG radionuclide therapy for neuroblastoma. J Nucl Med 2009; 50:1518–24.
45. Cristy M, Eckerman KF. Specific absorbed fractions of energy at various ages from internal photon sources. ORNL Health and Safety Research Division Report No. ORNL/TM-8381 V1-V7. Oak Ridge, TN: Oak Ridge National Laboratory; 1987. (http://bit.ly/2aNbfJw).
46. Livak KJ, Schmittgen TD. Analysis of relative gene expression data using real-time quantitative PCR and the 2(-delta delta C(T)) method. Methods 2001; 25:402–8.
47. R Core Team. R: A language and environment for statistical computing. Vienna, Austria: R Foundation for Statistical Computing; 2013.
48. Hänscheid H, Fernández M, Eberlein U, Lassmann M. Self-

irradiation of the blood from selected nuclides in nuclear medicine. Phys Med Biol 2014; 59:1515–31.

49. Flower MA, Fielding SL. Radiation dosimetry for therapy of neuroblastoma radiation dosimetry for neuroblastoma I-mIBG therapy of neuroblastoma. Phys Med Biol 1996; 41:1933–40.

50. Manning G, Kabacik S, Finnon P, Bouffler S, Badie C. High and low dose responses of transcriptional biomarkers in ex vivo X-irradiated human blood. Int J Radiat Biol 2013; 89:512–22.

51. Tucker JD, Divine GW, Grever WE, Thomas RA, Joiner MC, Smolinski JM, et al. Gene expression-based dosimetry by dose and time in mice following acute radiation exposure. PLoS One 2013; 8:e83390.